

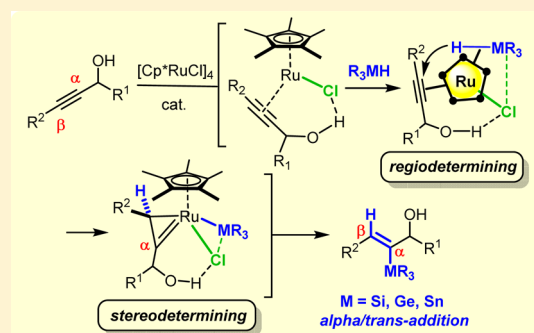
# Ruthenium-Catalyzed Alkyne *trans*-Hydrometalation: Mechanistic Insights and Preparative Implications

Dragoş-Adrian Roşca, Karin Radkowski, Larry M. Wolf,<sup>‡</sup> Minal Wagh,<sup>§</sup> Richard Goddard, Walter Thiel,<sup>Ⓛ</sup> and Alois Fürstner\*<sup>Ⓛ</sup>

Max-Planck-Institut für Kohlenforschung, D-45470 Mülheim/Ruhr, Germany

## Supporting Information

**ABSTRACT:**  $[\text{Cp}^*\text{RuCl}]_4$  (**1**) has previously been shown to be the precatalyst of choice for stereochemically unorthodox *trans*-hydrometalations of internal alkynes. Experimental and computational data now prove that the alkyne primarily acts as a four-electron donor ligand to the catalytically active metal fragment  $[\text{Cp}^*\text{RuCl}]$  but switches to adopt a two-electron donor character once the reagent  $\text{R}_3\text{MH}$  ( $\text{M} = \text{Si}, \text{Ge}, \text{Sn}$ ) enters the ligand sphere. In the stereodetermining step the resulting loaded complex evolves via an inner-sphere mechanism into a ruthenacyclopentene which swiftly transforms into the product. In accord with the low computed barriers, spectral and preparative data show that the reaction is not only possible but sometimes even favored at low temperatures. Importantly, such *trans*-hydrometalations are distinguished by excellent levels of regioselectivity when unsymmetrical alkynes are used that carry an  $-\text{OH}$  or  $-\text{NHR}$  group in vicinity of the triple bond. A nascent hydrogen bridge between the protic substituent and the polarized  $[\text{Ru}-\text{Cl}]$  unit imposes directionality onto the ligand sphere of the relevant intermediates, which ultimately accounts for the selective delivery of the  $\text{R}_3\text{M}-$  group to the acetylene C-atom proximal to the steering substituent. The interligand hydrogen bonding also allows site-selectivity to be harnessed in reactions of polyunsaturated compounds, since propargylic substrates bind more tightly than ordinary alkynes; even the electronically coupled triple bonds of conjugated 1,3-diyne can be faithfully discriminated as long as one of them is propargylic. Finally, properly positioned protic sites lead to a substantially increased substrate scope in that they render even 1,3-enynes, arylalkynes, and electron-rich alkynylated heterocycles amenable to *trans*-hydrometalation which are otherwise catalyst poisons.



## INTRODUCTION

Shortly after the turn of the millennium, Trost and co-workers reported that hydrosilylation reactions of internal alkynes switch from the canonical *cis*-addition<sup>1</sup> to an unorthodox *trans*-addition mode when catalyzed by  $[\text{Cp}^*\text{Ru}(\text{MeCN})_3]\text{PF}_6$ .<sup>2</sup> This remarkable discovery has opened access to structural motifs that are difficult to make otherwise. As a consequence, *trans*-hydrosilylation was rapidly embraced by the synthesis community,<sup>3,4</sup> despite the fact that nonsymmetrical substrates usually lead to the formation of regioisomers.<sup>5</sup>

Prompted by early applications of this methodology,<sup>6,7</sup> our group managed to expand the underlying principle in two dimensions: On one hand, we were able to impose the *trans*-addition mode<sup>8</sup> onto hydroboration,<sup>9</sup> hydrostannation,<sup>10,11</sup> hydrogermylation<sup>11,12</sup> and even hydrogenation reactions<sup>13–15</sup> of internal alkynes; all of these transformations seemingly violate reigning paradigms of organometallic chemistry and have little or no precedent in the literature. On the other hand, we could solve the regioselectivity problem for unsymmetrical substrates comprising a protic functional group in vicinity to the reacting triple bond. To this end, it suffices to replace the cationic precatalyst  $[\text{Cp}^*\text{Ru}(\text{MeCN})_3]\text{PF}_6$  used by Trost<sup>2,16</sup> by neutral ruthenium complexes featuring a  $[\text{Cp}^*\text{Ru}-\text{Cl}]$  motif in

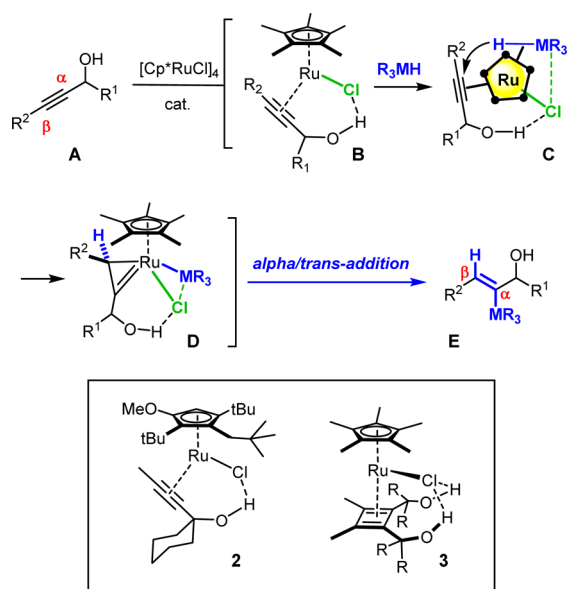
order to ensure faithful delivery of the  $\text{R}_3\text{M}$  unit ( $\text{M} = \text{Si}, \text{Ge}, \text{Sn}$ ) to the alkyne C-atom proximal to the steering substituent (Scheme 1).<sup>11,17</sup> This directing effect is particularly pronounced in *trans*-hydrostannation and has already served natural product total synthesis well.<sup>18,19</sup>

The synergy between a protic substituent on the substrate **A** and the polarized  $[\text{Ru}-\text{Cl}]$  bond of the catalyst was tentatively ascribed to interligand hydrogen bonding in adduct **B** primarily formed.<sup>11</sup> At the same time, the chloride aligns the incoming reagent via a hypervalent interaction with the  $-\text{MR}_3$  group. The resulting directionality within the ligand sphere of the loaded complex **C** explains the observed regioselectivity; subsequent inner-sphere hydride delivery forms a ruthenacyclopentene derivative of type **D** which accounts for the stereochemically intriguing *trans*-addition mode.<sup>11,20</sup>

This basic mechanistic scenario is in line with various pieces of indirect evidence, but all attempts at characterizing a complex of type **C** met with failure. Even the preceding alkyne adduct **B** could not be caught unless the  $\text{Cp}^*$  ring of the active catalyst was replaced by a much more encumbered and more

Received: December 5, 2016

Published: February 7, 2017

Scheme 1. Proposed Mechanism of Ruthenium-Catalyzed *trans*-Hydrometalation (● = CMe)

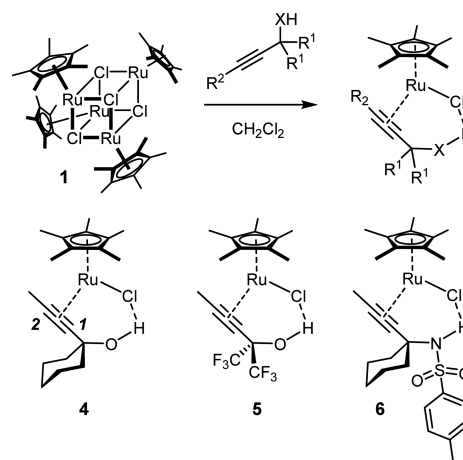
electron-rich  $\eta^5$ -1-methoxy-2,4-di-*tert*-butyl-3-neopentyl-cyclopentadienyl ( $Cp^*$ ) ligand;<sup>21</sup> only [2+2] cycloadducts were obtained as long as the  $Cp^*$  ring was in place.<sup>11</sup> Although the structural attributes of the model compound **2** and cycloadduct **3** are certainly in accord with our working hypothesis, they do not take away the need to investigate the real catalyst system in order to gain a better understanding for the origin and implications of this powerful steering effect ascribed to interligand interactions.

Outlined below is a comprehensive study along these lines. Specifically, we present a series of X-ray structures that reveal how prototype alkynes behave on coordination to the germane  $[Cp^*Ru-Cl]$  fragment. Adducts with ligands of different donor strength mimic the electronic response of such an alkyne complex to the incoming  $H-MR_3$  reagent ( $M = Si, Ge, Sn$ ). Moreover, spectral evidence indicates ready product formation once the loaded complex has formed and shows that product release is very facile. The gathered experimental data are correlated with computational results that provide insights into the peculiar bonding situation of  $[Cp^*RuCl(alkyne)]$  complexes formed at the outset and map the reaction coordinate, leading to the *trans*-addition product from there on. Moreover, it is shown that the virtues of interligand hydrogen bonding reach way beyond regiocontrol over  $H-MR_3$  delivery: notably, the effect allows acetylene derivatives of similar steric and/or electronic character to be distinguished with meaningful levels of selectivity; it even proves strong enough to invoke substrates that are otherwise inert.

## RESULTS AND DISCUSSION

**Hydroxyl-Assisted Alkyne Binding: Structural Data and Bonding Analysis.** Treatment of  $[Cp^*RuCl]_4$  (**1**)<sup>22</sup> as the standard catalyst for hydrometalations of all sorts with a *tert*-propargyl alcohol (1 equiv) leads to an instant color change from brown to cherry red (Scheme 2). NMR indicates clean formation of the corresponding  $\pi$ -complexes such as **4–6**, which are distinguished by massive deshielding of the alkyne C-atoms; the observed downfield shift  $\Delta\delta$  is in the order of  $\sim 50$ – $70$  ppm (Table 1). This immense effect is best explained by

Scheme 2. Formation of Alkyne Complexes Suitable for X-ray Diffraction



assuming that both orthogonal acetylenic  $\pi$ -systems engage in bonding; if the substrate serves as a four-electron donor,<sup>23,24</sup> the resulting complex gains a formal 18-electron count. At the same time, the  $-OH$  proton experiences significant deshielding, indicative of interligand hydrogen bonding.

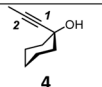
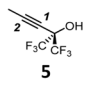

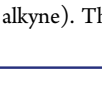


Although adduct formation is fast and clean according to NMR, our early attempts at isolating the resulting  $\pi$ -complexes had met with failure; as mentioned above, only downstream [2+2] cycloadducts such as **3** had been obtained.<sup>11,25</sup> It was only after considerable experimentation that our efforts were finally rewarded with success. Specifically, single crystals suitable for X-ray diffraction could be grown from the representative complexes **4–6** comprising a propargyl alcohol or a propargylic sulfonamide, respectively (Figure 1 and Figures S2 and S3 in the Supporting Information).

While the gross structural attributes of these complexes are similar, the differences in details are arguably telling. In all cases is  $\pi$ -complex formation supported by peripheral hydrogen bonding between the protic substituent and the chloride atom as inferred from  $^1H$  NMR.<sup>26</sup> The strength of this contact seems correlated with the acidity of the protic group, in that the  $-X(H)\cdots Cl$  bond length increases from a short 2.975(1) Å in **5**, bearing two electron-withdrawing  $-CF_3$  groups, to 3.072(3) Å in **4**, comprising an “ordinary” propargyl alcohol, to 3.153(2) Å in the sulfonamide adduct **6**; yet, even this distance must be rated “short” and “strong” according to the categories of organometallic chemistry.<sup>27</sup> Whereas the protons engaged in hydrogen bonding are less well located in the X-ray analyses, the differences in the  $-X\cdots Cl$  distances can be considered significant.

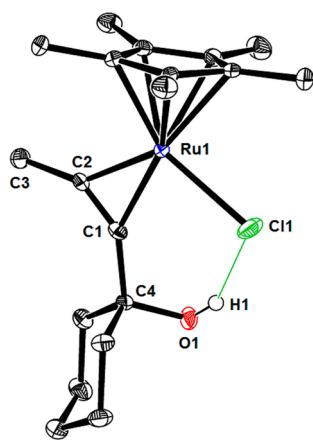
A closer inspection of the bound alkyne is equally informative. The substantial elongation of the  $C\equiv C$  bond<sup>28</sup> indicates a high degree of activation which is qualitatively in line with the massive deshielding observed by  $^{13}C$  NMR. Interestingly, the  $C\equiv C$  bond in **5** (1.283(1) Å) is longer than that in **4** (1.264(4) Å) and the alkyne slightly more bent away from linearity ( $C3-C2-C1$  144.75(8)° versus 145.3(3)°). This geometric attribute reveals non-negligible electron back-donation from the filled d-orbitals of the metal into the  $\pi^*$ -orbitals of the bound alkyne, which becomes stronger upon lowering the LUMO level by virtue of the electron withdrawing fluorine atoms in **5**.

The qualitative conclusion drawn from the experimental data that strong four-electron donation from the alkyne to the metal

Table 1. Characteristic Spectral Data ( $\text{CD}_2\text{Cl}_2$ , ppm) of Representative Free Alkynes and the Corresponding Complexes 4–6

Compound	$\delta_{\text{H}} (\text{OH/NH})$	$\Delta\delta^{[a]}$	$\delta_{\text{C}} (\text{C1})$	$\Delta\delta$	$\delta_{\text{C}} (\text{C2})$	$\Delta\delta^{[a]}$
	1.88	3.19	83.6	71.1	80.0	50.0
	5.07		154.7		130.1	
	4.90	3.13	87.8	54.5	69.0	67.0
	8.03		142.3		136.3	
	4.74	2.27	80.9	65.6	78.3	61.9
	7.01		146.5		140.2	

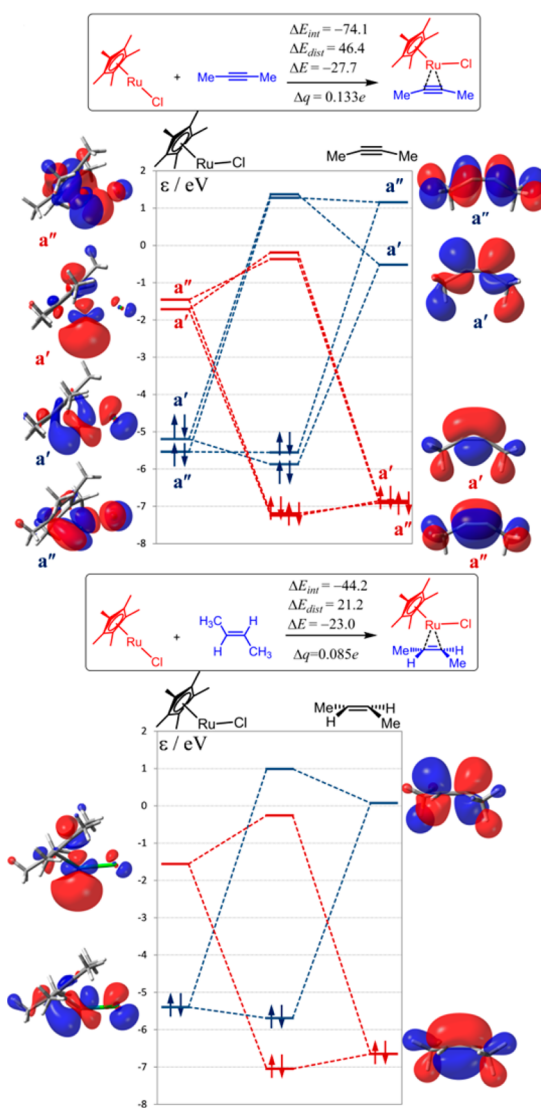
<sup>a</sup> $\Delta\delta = \delta(\pi\text{-complex}) - \delta(\text{free alkyne})$ . The numbering scheme for the alkyne C-atoms is as shown in Scheme 2 and the X-ray structures; arbitrary numbering as indicated.



**Figure 1.** Structure of complex 4 in the solid state; all H-atoms, except the one engaged in hydrogen bonding to the chloride ligand, are omitted for clarity; only one of the two independent molecules in the unit cell is shown; for the X-ray structures of complexes 5 and 6, see the Supporting Information.

goes hand in hand with non-negligible back-bonding is substantiated by the orbital interaction diagram constructed using orbital perturbation theory at the M06/TZ2P level (Figure 2).<sup>29</sup> The strongest interaction in the model complex  $[\text{Cp}^*\text{Ru}(\text{Cl})(\text{CH}_3\text{C}\equiv\text{CCH}_3)]$  results from the  $\sigma$ -symmetric electron donation from the  $[\text{Cp}^*\text{RuCl}]$  fragment HOMO( $a'$ ) of largely  $d_z^2$  character. This interaction is strongest with the alkyne carbon that is distal to the Cl ligand (proximal to the  $\text{Cp}^*$ ) due to the orbital directionality. The  $[\text{Cp}^*\text{RuCl}]$  HOMO-1( $a''$ ) is of similar energy but only overlaps slightly with the alkyne LUMO+1( $a''$ ). The  $[\text{Cp}^*\text{RuCl}]$  LUMO( $a'$ ), mostly of  $5s$  character, and LUMO-1( $a''$ ) experience  $\sigma$ - and  $\pi$ -symmetric electron donation from both  $\pi$ -clouds ( $a'$  and  $a''$ , respectively). The summation of both  $\pi$ -cloud donations is slightly greater than the donation from the  $[\text{Cp}^*\text{RuCl}]$  HOMO. The charge transfer from complexation amounts to a net charge transfer of  $\Delta q = 0.133e$  from the ligated alkyne to the  $[\text{Cp}^*\text{RuCl}]$  fragment. Therefore, it seems justified to qualitatively rate the alkyne as a four-electron donor.

Additional support for the alkyne four-electron donor behavior comes from comparison to the analogous alkene complex  $[\text{Cp}^*\text{Ru}(\text{Cl})(\text{trans-2-butene})]$ . The enhanced distortion in the alkyne relative to the alkene is caused by the greater orbital interactions within  $[\text{Cp}^*\text{Ru}(\text{Cl})(\text{CH}_3\text{C}\equiv\text{CCH}_3)]$  as compared with  $[\text{Cp}^*\text{Ru}(\text{Cl})(\text{trans-2-butene})]$ .



**Figure 2.** Orbital diagram of the model complexes  $[\text{Cp}^*\text{Ru}(\text{Cl})(\text{CH}_3\text{C}\equiv\text{CCH}_3)]$  (top) and  $[\text{Cp}^*\text{Ru}(\text{Cl})(\text{trans-2-butene})]$  (bottom) computed at the M06/TZ2P level. The binding energy  $\Delta E$  is the sum of the interaction energy  $\Delta E_{\text{int}}$  and the distortion energy  $\Delta E_{\text{dist}}$  (given in  $\text{kcal mol}^{-1}$ ); charge transfers ( $\Delta q$ ) are computed from NBO partial atomic charges, see the Supporting Information.

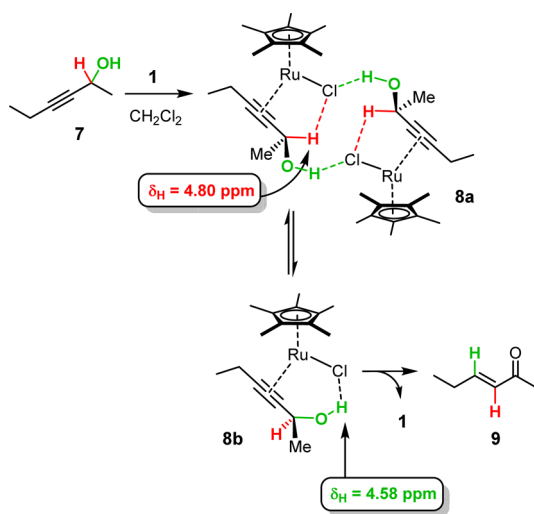
The alkene has only one  $\pi$ -cloud donor which is nearly offset by the back-donation from the  $[\text{Cp}^*\text{RuCl}]$  HOMO.

Furthermore, the computed complexation induced charge transfer is computed to be  $\Delta q = 0.085e$ , which is less than with the alkyne complexed, consistent with the reduced donation from the ligand  $\pi$  framework.

The orbital schemes for bound propargyl alcohol are basically identical, as are the computed bond lengths. This result shows that the presence of a hydroxyl group in the substrate able of entertaining an interligand hydrogen bond does not change the orbital interactions and hence the intrinsic reactivity of the resulting  $\pi$ -complex; however, it is computed to increase its stability by  $\sim 2.8$ – $4.8$  kcal/mol, depending on the particular substrate (*vide infra*). As will be shown below, this differential allows otherwise unreactive substrates to be processed and/or site selectivity to be imposed on *trans*-hydrometalation reaction of various diyne derivatives.

**Secondary Propargyl Alcohols: Competing Redox Isomerization.** The preparation of complexes **4** and **5** comprising *tert*-propargyl alcohols as ligands had proven taxing, but the isolation of the analogous complex **8** carrying a *sec*-propargyl alcohol was even more difficult (Scheme 3). The

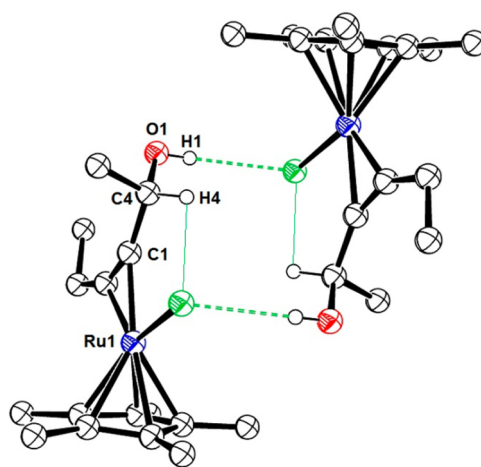
### Scheme 3. Coordination Behavior of a Secondary Propargyl Alcohol



additional challenge arises from the propensity of such substrates to undergo redox isomerization with formation of the corresponding enones even at low temperature.<sup>30,31</sup> It was only after considerable experimentation that single crystals of **8** suitable for X-ray diffraction could be grown, which must be kept cold at all time to avoid instantaneous formation of hex-3-en-5-one (**9**) and regeneration of  $[\text{Cp}^*\text{RuCl}]_4$  (**1**).

The bonding of the alkyne unit to the metal fragment in **8** is very similar to that in **4** or **5**. This is evident from the massive downfield shift of the ligated C-atoms in the  $^{13}\text{C}$  NMR spectrum ( $\delta_{\text{C}} = 150.7/135.5$  ppm versus 85.4/81.3 ppm in the free alkyne), the elongation of the triple bond (1.268(3) Å), and the significant bending of the acetylene unit (C4–C1–C2 147.0(10)°).

The arguably most striking feature of **8** is the now *intermolecular* hydrogen-bonding pattern between the –OH group and the chloride ligand of the next unit at an –O–(H)⋯Cl distance of 3.12(3) Å (average of two crystal forms, see the SI) (Figure 3). As if to compensate, the hydrogen atom H4 at the foot of the propargylic alcohol unit makes a rather short intramolecular contact with the neighboring chloride (–C–



**Figure 3.** Structure of complex **8** in the solid state featuring an intermolecular hydrogen-bonding pattern between two monomer units; all H-atoms, except the ones engaged with the chlorides, are omitted for clarity.

(H)⋯Cl, 3.22(4) Å). Since 1,2-shift of this particular H-atom entails redox isomerization, it is tempting to assume that this step might enjoy assistance by the flanking chloride too. In line with this notion, H4 in complex **8** ( $\delta_{\text{H}} = 4.80$  ppm) resonates downfield from the proton in the unbound substrate ( $\delta_{\text{H}} = 4.45$  ppm), which suggests that a weak interaction persists in solution. An equilibrium with a second conformer **8b** is reasonable; this assumption is based on the characteristic deshielding of the –OH proton which persists even at low concentrations at which intermolecular contacts are highly unlikely. In any case, the downfield shift of H4 speaks against a developing hydridic character and hence against a mechanism of redox isomerization via simple 1,2-hydride transfer. In this context, it should be noted that related interactions between the [Ru–Cl] unit and the  $\text{R}_3\text{M}$  group (M = Si, Ge, Sn) are crucial for *trans*-hydrometalations to proceed.<sup>11</sup> Therefore, it seems legitimate to assume that ruthenium catalyzed redox isomerization, *trans*-hydrometalations and *trans*-hydrogenation—in their essence—are different manifestations of the same fundamental reactivity mode.

If a *tertiary* propargyl alcohol (amide), when ligated to  $[\text{Cp}^*\text{RuCl}]$ , were to entertain an intermolecular hydrogen-bonding pattern as manifest in **8a**, a clash between the chloride and one of the carbon substituents would ensue (R instead of the H-atom labeled in red in Scheme 3). To avoid such penalty, these substrates strongly favor the intramolecular hydrogen-bonding mode seen in the X-ray structures of **4** and **5**, which corresponds to conformer **8b**. This “Thorpe–Ingold effect” translates into particularly effective regiocontrol in the subsequent *trans*-hydrometalation. Experimental results from our group indeed show the somewhat counterintuitive trend that delivery of the bulky  $\text{R}_3\text{M}$  group to the proximal C-atom becomes more selective when going from a secondary (or primary) to an arguably more encumbered tertiary propargyl alcohol substrate. The examples compiled in Table 2 are representative.<sup>11</sup>

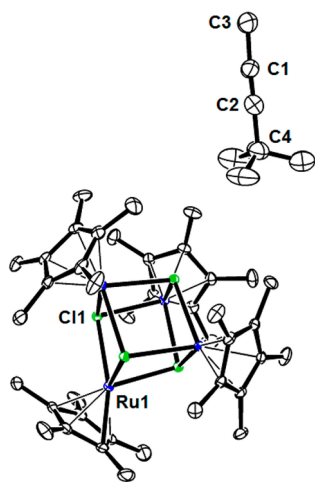
**Binding of an Unfunctionalized Alkyne.** The computational data outlined above show that a protic site in vicinity to the triple bond does not change the bonding interactions with the  $[\text{Cp}^*\text{Ru–Cl}]$  fragment *per se* but markedly enhances the stability of the resulting complex. To confirm this important

**Table 2.** Comparison of the Regioselectivity of *trans*-Hydrometalation Reactions of Prototype Secondary and Tertiary Propargyl Alcohol Substrates Catalyzed by **1** (1.25 mol%)<sup>11</sup>

Entry	Substrate	R <sub>3</sub> MH	solvent	proximal:distal	Yield (%)
1		BnMe <sub>2</sub> SiH	pentane	88:12	95
2		Et <sub>3</sub> SiH	pentane	91:9	86
3		Bu <sub>3</sub> SnH	CH <sub>2</sub> Cl <sub>2</sub>	93:7	89
4		BnMe <sub>2</sub> SiH	pentane	≥ 99:1	92
5		Et <sub>3</sub> SiH	pentane	≥ 99:1	99
6		Bu <sub>3</sub> SnH	CH <sub>2</sub> Cl <sub>2</sub>	≥ 99:1	94

conclusion, binding studies with an unfunctionalized substrate of similar steric demand were carried out.

Attempted crystallization of an adduct between 4,4-dimethyl-2-pentyne (**10**) and complex **1** have so far met with failure. Rather, the single crystals precipitating from a concentrated solution in CH<sub>2</sub>Cl<sub>2</sub> at  $-20\text{ }^{\circ}\text{C}$  solely consisted of unchanged [Cp\**Ru*Cl]<sub>4</sub> and solute 4,4-dimethyl-2-pentyne (Figure 4). The triple bond is unperturbed (1.168(5) Å) and the alkyne almost linear (C3–C1–C2 175.4(4)<sup>o</sup>).

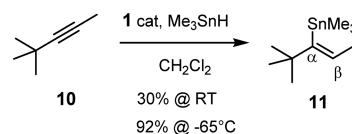


**Figure 4.** Asymmetric unit of the cocrystals formed from **1** and 4,4-dimethyl-2-pentyne (**10**).

Further cooling of a more dilute solution in CD<sub>2</sub>Cl<sub>2</sub>, however, led to a characteristic color change from brown to purple. According to NMR, 70% of **10** is bound to the metal fragment at  $-50\text{ }^{\circ}\text{C}$ ; cooling/warming cycles proved the process to be fully reversible. As expected, the C-atoms of bound **10** show the same characteristic deshielding ( $\delta_{\text{C}} = 159.4, 131.1\text{ ppm}$ ) as those of the propargylic substrates discussed in the previous sections.

These data prove that substrates with and without protic functionality bind in the same way to the catalytically active [Cp\**Ru*Cl] fragment and therefore undergo the same *trans*-addition reactions; however, they exhibit largely different affinities. In a preparative context this distinction can be turned into an advantage as it allows propargyl alcohols to be addressed without touching an “ordinary” alkyne in vicinity (see below). Furthermore, hydrometalations of substrates with low binding affinity have a better chance to proceed when carried out at low temperatures, provided the R<sub>3</sub>MH reagent is added slowly to avoid competing decomposition of the catalyst. The example shown in Scheme 4 is representative: Whereas the *trans*-hydrostannation of the bulky substrate **10** under the

**Scheme 4.** *trans*-Hydrostannation of **10** at Low Temperature<sup>a</sup>

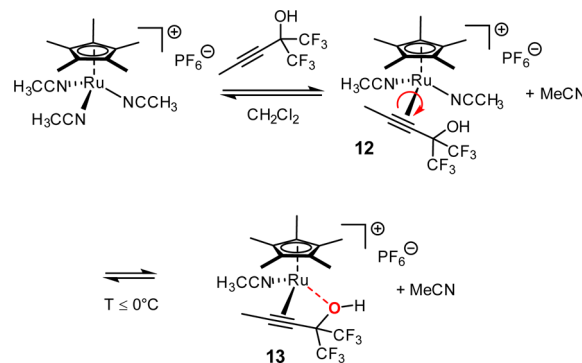


<sup>a</sup>Successful transformation, however, requires slow addition to avoid decomposition of the precatalyst by excess stannane; product **11** formed at  $-65\text{ }^{\circ}\text{C}$  was  $\sim 95\%$  isomerically pure.

standard conditions at ambient temperature gave poor results, the same reaction carried out at  $-65\text{ }^{\circ}\text{C}$  afforded the desired product **11** in appreciable yield. The major isomer results from hydride delivery to the less hindered acetylene C-atom; this preference leads to the somewhat counterintuitive but potentially very useful substitution pattern in which the bulky Me<sub>3</sub>Sn residue ends up adjacent to rather than distal from the bulky *tert*-butyl group.

**Binding to Cationic Catalysts.** If a peripheral hydrogen bond with a Ru–Cl unit stabilizes an alkyne  $\pi$ -complex by  $\sim 2.8\text{--}4.8\text{ kcal/mol}$ , the halide-free cationic catalyst [Cp\**Ru*(MeCN)<sub>3</sub>]<sup>+</sup>PF<sub>6</sub><sup>−</sup> originally used by Trost and co-workers for *trans*-hydrosilylation<sup>2,16</sup> should bind a propargyl alcohol derivative much less tightly than [Cp\**Ru*Cl]<sub>4</sub>. This is indeed the case: according to <sup>19</sup>F NMR, only 16% of 1,1,1-trifluoro-2(2-trifluoromethyl)pent-3-yn-2-ol are bound to the cationic template at  $-50\text{ }^{\circ}\text{C}$  (Scheme 5).<sup>32</sup> Interestingly though, the

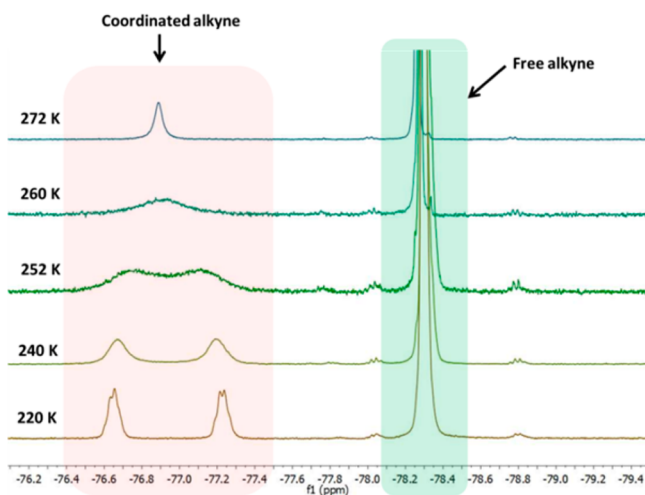
**Scheme 5.** Temperature-Dependent Coordination of a Propargyl Alcohol to a Cationic [Cp\**Ru*]<sup>+</sup> Fragment



CF<sub>3</sub> groups are diastereotopic at this low temperature, which likely indicates that a chelate structure **13** is formed by coordination of the –OH group to the metal center (Figure 5).<sup>33</sup> Determination of the coalescence temperature and line shape analysis reveal a low barrier between **12** and **13** ( $\Delta H^{\ddagger} \approx 6\text{ kcal/mol}$ ) and an associative pathway for chelate formation/displacement of MeCN ( $\Delta S^{\ddagger} = -22.4\text{ cal}\cdot\text{mol}^{-1}\cdot\text{K}^{-1}$ ).

**Attempted Characterization of the Loaded Catalyst.** The data outlined above leave no doubt that the polarized [Ru–Cl] unit is key for the preorganization of the ligand sphere of the catalyst in that it locks the alkyne substrate via interligand hydrogen bonding. At the same time, a hypervalent Cl⋯MR<sub>3</sub> interaction has been proposed to position the incoming reagent H–MR<sub>3</sub> in a matching orientation to give a loaded complex of type C as the key intermediate accountable for regio- and stereoselective *trans*-hydrometalation.<sup>11</sup>

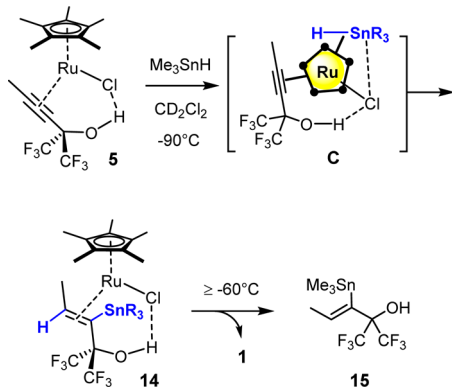
In an attempt to verify this scenario, Me<sub>3</sub>SnH was quickly added to a cherry-red solution of the well-defined alkyne adduct



**Figure 5.** Variable-temperature  $^{19}\text{F}$  NMR spectrum ( $\text{CD}_2\text{Cl}_2$ ) of a 1:1 mixture of  $[\text{Cp}^*\text{Ru}(\text{MeCN})_3]\text{PF}_6$  and 1,1,1-trifluoro-2-(2-trifluoromethyl)pent-3-yn-2-ol.

**5** in  $\text{CD}_2\text{Cl}_2$  at  $-90^\circ\text{C}$ , causing an instant color change to purple (**Scheme 6**). A single new species is formed according to

**Scheme 6. Attempted Characterization of a Loaded Complex Proves That *trans*-Hydrostannylation Is Facile Even at Low Temperatures**



NMR; however, it is not the loaded complex **C** but the ruthenium adduct of the hydrostannylated alkene product. The fact that hydrogen and tin are *trans* to each other in the alkene ligand of complex **14** even when formed at very low temperature rules out the possibility that the unorthodox stereochemical outcome is no more but the net result of a conventional *cis*-addition followed by isomerization;<sup>1</sup> rather, this observation constitutes the most rigorous experimental proof so far that *trans*-addition is truly an inherent quality.

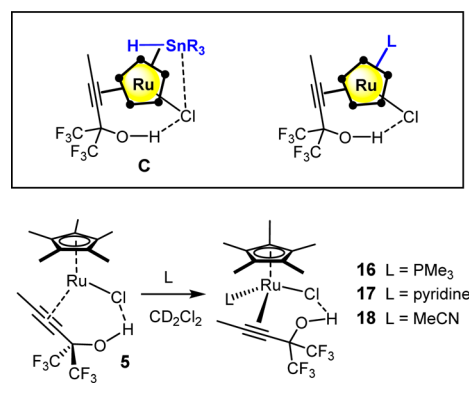
Even gentle warming of the solution of **14** to  $-60^\circ\text{C}$  suffices to release product **15** and  $[\text{Cp}^*\text{RuCl}]_4$  (**1**); this step is irreversible within the limits of detection of NMR, thus showing that the alkene product is a much weaker ligand than the alkyne substrate. Associated with this is a characteristic change of the  $^3J_{\text{Sn,H}}$ , which increases from 88 Hz in **14** to 124 Hz in **15**: this feature indicates substantial rehybridization during decomplexation, which in turn implies significant electron back-donation from the Ru center into the  $\pi^*$ -orbital of the alkene in adduct **14**. This finding concurs with the computational results for *trans*-2-butene outlined above. The ready formation of the product and its facile decomplexation

even at low temperatures implies a favorable reaction coordinate with only low barriers once the loaded  $\pi$ -complex has formed; this is well in line with the computational results outlined below. The argument is reinforced by the fact that the *trans*-hydrostannylation of 4,4-dimethyl-2-pentyne (**10**) was also successful at  $-65^\circ\text{C}$ , as long as the stannane was added slowly (**Scheme 4**).

**Emulation of the Loaded Catalyst.** The gathered data leave no doubt that an alkyne substrate, when bound to  $[\text{Cp}^*\text{RuCl}]$ , acts as a four-electron donor in the first place. The empirical 18-electron rule, however, mandates that it mutates to a two-electron donor when  $\text{H-MR}_3$  is taken up and a conceived intermediate of type **C** is formed (**Scheme 1**). If this switch of the donor character does not occur, the proposed inner sphere mechanism is obsolete. The fact that **C** could not be observed by NMR even at  $-90^\circ\text{C}$  might either mean that it is too short-lived for direct inspection or that it does not form at all.

To clarify this critical aspect, attempts were made to emulate the loaded catalyst by formal replacement of  $\text{H-MR}_3$  by nonreactive donor ligands (**Scheme 7**). In a first foray,  $\text{Me}_3\text{P}$

**Scheme 7. Emulation of the Loaded Complex**



was added to a solution of complex **5** in  $\text{CD}_2\text{Cl}_2$  at  $-78^\circ\text{C}$ , which engenders a pronounced upfield shift of the acetylene signals. The alkyne resonances in the resulting product **16** are very close to those of the unbound substrates (**Table 3**). The fact that the  $^{13}\text{C}$  NMR signals show characteristic  $^2J_{\text{P,C}}$  couplings, however, proves that the alkyne remains bound and has not been displaced from the metal center by the phosphine. This aspect is also manifest in the diastereotopic character of the two  $\text{CF}_3$  groups in complex **16**.

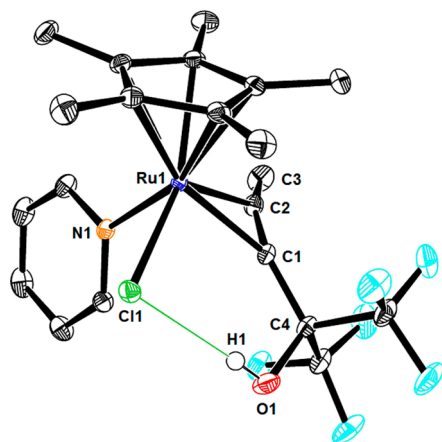
Weaker  $\sigma$ -donor ligands such as pyridine or MeCN entail similar effects, even though the resulting adducts are more labile and coordination is (fully) reversible.<sup>34</sup> In the case of **17**, the two  $\text{CF}_3$  groups display a singlet resonance at RT but resolve to two quartets at  $-50^\circ\text{C}$ . For **18**, the singlet  $\text{CF}_3$  resonance begins to split only at  $-85^\circ\text{C}$  and full resolution could not be reached above the freezing point of the solvent ( $-96.7^\circ\text{C}$ ).

Adducts **16** (Figure S7, **Supporting Information**) and **17** (Figure 6) have also been characterized by X-ray diffraction. It is interesting to note that the switch of the acetylene from a four- to a two-electron donor—as clearly expressed in the NMR data (**Table 3**)—is not reflected in the  $\text{C}\equiv\text{C}$  bond lengths that remain long (1.256(3) and 1.260(1) Å, respectively); likewise, a significant bending of the alkyne away from linearity persists in either case. Obviously, electron

Table 3. Characteristic  $^{13}\text{C}$  NMR Data ( $\text{CD}_2\text{Cl}_2$ , ppm)

Compound	$\delta(\text{C1})$ (ppm)	$\delta(\text{C2})$ (ppm)
	87.8	69.0
	142.3	136.3
	89.9 ( $J_{\text{PC}} = 8.4$ Hz)	71.9 ( $J_{\text{PC}} = 6.7$ Hz)
	n.d. <sup>[a]</sup>	n.d. <sup>[a]</sup>

<sup>a</sup>Not detected because of massive line broadening caused by fast MeCN exchange even at  $-85$  °C.



**Figure 6.** Structure of complex **17** in the solid state; all H-atoms, except the one engaged in hydrogen bonding to the chloride ligand, are omitted for clarity. For the X-ray structure of the corresponding phosphine adduct **16**, see the [Supporting Information](#).

back-donation from  $[\text{Cp}^*\text{Ru}]$  to the antibonding  $\pi^*$ -orbital as the major determining factor of either structural attribute is operative independent of whether the alkyne acts as a four- or two-electron donor ligand. While the  $\text{Ru1}-\text{P1}$  bond in **16** is rather short (2.299(9) Å), the  $\text{Ru1}\cdots\text{N1}$  distance (2.157(1) Å) in the pyridine adduct **17** is well above the sum of the van der Waals radii (2.01 Å), indicative of an only weak interaction even in the solid state. Importantly, the peripheral interligand  $-\text{O}-(\text{H})\cdots\text{Cl}$  hydrogen bonding persists in either adduct although it is slightly longer than that in **5** (2.975(1) Å) [(3.039(3) Å in complex **16**; 3.044(1) Å in complex **17**]. Nevertheless, the bridges remain strong enough to lock the propargyl alcohol in place.<sup>27</sup>

These data showcase that ligands of different donor ability readily enter into the coordination sphere of an alkyne complex of type **B**; reagents of type  $\text{H}-\text{MR}_3$  are expected to do the same as they are known to form well-defined  $\sigma$ -stannane or  $\sigma$ -

silane complexes with  $[\text{Cp}^*\text{RuCl}]$  fragments.<sup>11,35–37</sup> Although the gathered information is no rigorous proof, it is definitely in accord with the proposed inner sphere mechanism involving a loaded complex of type **C**. Qualitatively, electron donation from the metal fragment to the ligated  $\text{R}_3\text{M}-\text{H}$  bond increases the hydridic character and should hence render addition to the activated triple bond more facile.

**Computational Studies.** While all experimental data speak for an inner-sphere rather than an outer-sphere mechanism, this aspect was deemed sufficiently important to warrant further scrutiny. Therefore, a detailed computational study of *trans*-hydrostannation was carried out at the SMD(DCM)-M06/def2-TZVP//M06/def2-SVP level of theory (see [Supporting Information](#) for details), which complements earlier investigations on *trans*-hydrosilylation<sup>20</sup> as well as *trans*-hydrogenation.<sup>15</sup> The focus on *trans*-hydrostannation seems legitimate given its particularly wide scope and excellent selectivity.<sup>10,11,18,19</sup>

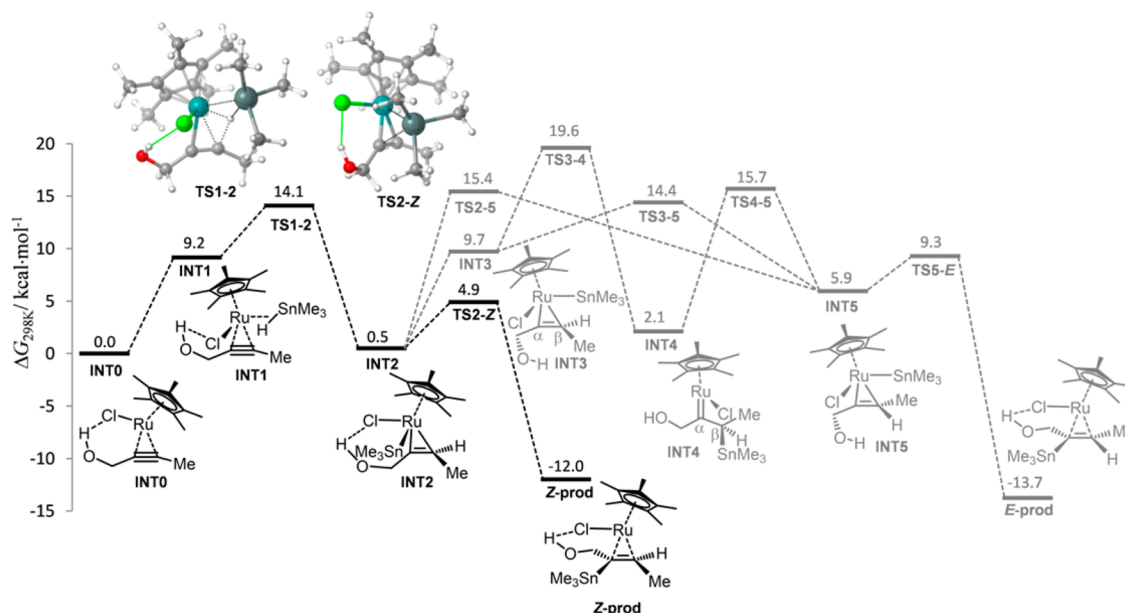
In excellent agreement with the experimental data, binding of a propargyl alcohol to the metal fragment affords a complex with a peripheral interligand hydrogen bond, which is capable of binding  $\text{Me}_3\text{SnH}$  in the form of the  $\sigma$ -complex **INT1** ([Figure 7](#)). This starting point corresponds to complex **C** that we had proposed in this and our earlier experimental work.<sup>11</sup> The ruthenium center in **INT1** cleaves the  $\text{Sn}-\text{H}$  bond while transferring the hydride to the ligated butynol substrate in a concerted fashion via **TS1-2** ( $\Delta G^\circ = 4.9$  kcal/mol). The resulting metallacyclopentene ( $\eta^2$ -vinylruthenium)<sup>38</sup> intermediate **INT2** undergoes direct reductive elimination of the  $\text{Me}_3\text{Sn}$ -group to the “carbene-type”  $\alpha$ -center to form the *trans*-addition product via **TS2-Z** with a barrier of only 4.4 kcal/mol. This route is by far the lowest energy pathway available to **INT2** and leads to the experimentally observed *trans*/ $\alpha$ -product (**Z-prod**,  $-21.1$  kcal/mol).

Evolution of **INT2** into the thermodynamically slightly more stable *cis*/ $\alpha$ -product (**E-prod**,  $-22.9$  kcal/mol) is possible by either a concerted (via **TS2-5**) or a stepwise pathway (via **INT3** and **TS3-5**) to give the isomeric ruthenacyclopentene **INT5**, which forms the product upon reductive coupling. Even the more favorable of these two possible routes, however, is 9.5 kcal/mol higher in energy than the pathway leading to the *trans*/ $\alpha$ -product. This differential finds excellent correspondence in the generally very high levels of selectivity observed in such reactions.<sup>11,18,19</sup>

Unlike the *trans*-hydrogenation of alkynes,<sup>15</sup> where the evolution of the ruthenacyclopentene into a true carbene constitutes an important additional reaction channel, the formation of an analogous carbene **INT4** by reductive elimination of the tin residue and the  $\text{Ru}-\text{C}_\beta$  bond proved highly unfavorable. **INT4** could derive from **INT3** passed through en route to the *cis*-addition product, but the barrier to its formation is prohibitively high.

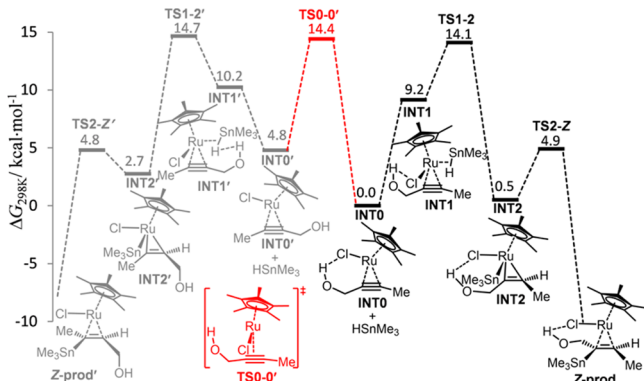
Attempts at finding pathways in which  $\text{Me}_3\text{Sn}$  delivery precedes hydrogen transfer met with failure; they invariably converged to the “hydrogen first” route shown in [Figure 7](#). This preference distinguishes the hydrostannation from hydrosilylation, for which  $\text{Me}_3\text{Si}$  transfer prior to H transfer is feasible.<sup>20</sup> The distinct behavior manifest in these computational data, however, is quite intuitive if one considers that  $\sigma$ -stannane complexes are certainly more hydridic than their  $\sigma$ -silane counterparts.

Possible stannation of the distal C-atom was also investigated to determine if hydrogen bonding could effectively account for



**Figure 7.** Computed Gibbs free energy profile of a prototype hydrostannation catalyzed by  $[\text{Cp}^*\text{RuCl}]$  in  $\text{CH}_2\text{Cl}_2$ ; energies in kcal/mol.

the regioselectivity (Figure 8). Indeed association of the alkyne leads to an association complex  $\text{INT0}'$  that is higher in energy



**Figure 8.** Computed Gibbs free energy profile in  $\text{CH}_2\text{Cl}_2$  (in units of kcal/mol) for distinguishing distal/proximal hydrostannation of a prototype propargyl alcohol.

than the  $\text{INT0}$  containing the hydrogen bond by 4.8 kcal/mol. The barrier height of their interconversion ( $\text{TS0-0}'$ ) is similar in magnitude to the highest barrier heights leading to the stereoisomeric products  $\text{Z-prod}$  and  $\text{Z-prod}'$  suggesting that the product selectivity depends largely on the energy difference between  $\text{INT0}$  and  $\text{INT0}'$ . The energy difference between the  $\text{HSnMe}_3$  association complexes  $\text{INT1}$  and  $\text{INT1}'$  is smaller due to a hydrogen bond with the complexed hydride in  $\text{INT1}'$ . Overall, this result is in agreement with the experimentally observed preference for the proximal product,  $\text{Z-prod}$ .

**Preparative Implications.** *trans*-Hydrometalations as well as *trans*-hydrogenation have proven difficult, if not impossible, for all substrates that contain structural elements competing with the alkyne unit for binding to the active ruthenium fragments  $[\text{Cp}^*\text{Ru}]^+$  or  $[\text{Cp}^*\text{RuCl}]$ ; all potential four- or six-electron donors fall into this category.<sup>39–41</sup> That is why problems are frequently encountered when working with starting materials that comprise an (electron-rich) arene and/

or a 1,3-diene unit; likewise, 1,3-enynes also usually fail to react. Compounds **19–24** are representative (Scheme 8).<sup>10,11</sup>

We reasoned that this shortcoming might be remedied, at least in part, with the help of appropriately positioned protic substituents (Scheme 8). While a regular enyne **F** likely traps

**Scheme 8. (Top) Representative Examples of Poorly Reactive Substrates Comprising Four-/Six-Electron Donor Sites; (Bottom) The Presence of a Protic Group in the Vicinity of the Alkyne Might Allow a Reactive Binding Mode To Be Achieved and Hence the Substrate Scope To Be Increased**

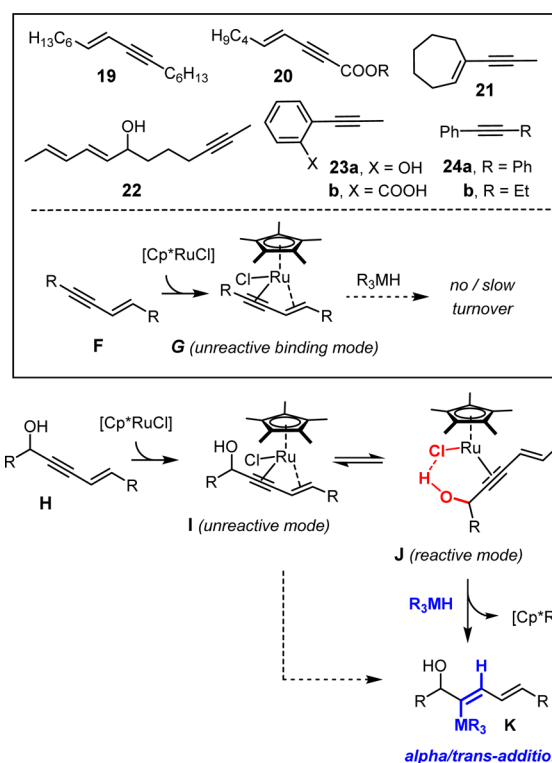




Table 4. *trans*-Hydrostannations of Substrates Containing a Protic Site Next to a 1,3-Enyne or Arene Unit<sup>a</sup>

Entry	Substrate	Major product	proximal: distal <sup>b</sup>	Yield (%)
1			99:1 <sup>c</sup>	60 <sup>d</sup>
2			96:4	72 <sup>d,e</sup>
3			98:2	64
4			>95:5	60 <sup>d,e</sup>
5			>95:5	82 <sup>d</sup>
6			93:7	66 <sup>d</sup>
7			99:1	87 (R = TBS) <sup>f</sup>
8			99:1	95 (R = TMS) <sup>f</sup>
9			[g]	55 <sup>d</sup>
10			95:5	86 <sup>f,h</sup>
11			>95:5	90
12			99:1	55
13			>95:5	72 <sup>i</sup>
14			[j]	74

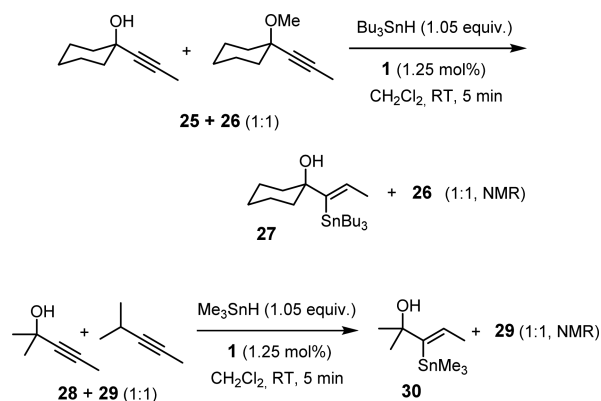
<sup>a</sup>The reactions were carried out at ambient temperature with 1.05–1.2 equiv of R<sub>3</sub>SnH in CH<sub>2</sub>Cl<sub>2</sub> in the presence of **1** (1–2 mol %); unless stated otherwise, the selectivity for *trans*-addition was ≥95:5 (major regioisomer). <sup>b</sup>“Proximal” denotes delivery of the R<sub>3</sub>M group to the alkyne C-atom next to the protic group, whereas “distal” refers to the more remote C-atom. <sup>c</sup>Z:E = 87:13 (major isomer). <sup>d</sup>Yield of pure *trans*/α-product after flash chromatography. <sup>e</sup>Using [Cp\**2*RuCl<sub>2</sub>]<sub>n</sub> as the catalyst. <sup>f</sup>Traces of distannylated product were detected. <sup>g</sup>The crude product contains other isomers that were not rigorously assigned. <sup>h</sup>At –30 °C. <sup>i</sup>At –10 °C. <sup>j</sup>Ca. 20% distannylated product was formed. For the sake of a better overview, the table includes some examples from our previous work.<sup>11,19</sup>

the catalyst in the form of stable adducts of type **G**, the steering effect of a propargylic –OH group might allow a compound of type **H** to reach a reactive coordination mode **J** and hence *trans*-addition to proceed. Similar arguments can be given for ordinary arylalkynes and their hydroxylated siblings, respectively.

In line with this notion, the examples compiled in Table 4 (entries 1–6) show that adequately functionalized 1,3-enynes are indeed amenable to *trans*-hydrostannation, whereas their unfunctionalized relatives **19**–**21** (Scheme 8) basically fail to react. The presumed steering effect responsible for this favorable outcome definitely surfaces in the high preference for proximal R<sub>3</sub>M delivery in all cases investigated.

The higher affinity of propargyl alcohols to [Cp\**2*RuCl] also allows meaningful levels of site-selectivity to be harnessed in reactions of polyunsaturated substrates. This is manifest in the intermolecular competition experiments shown in Scheme 9, in which an unprotected propargyl alcohol clearly wins over the corresponding methyl ether as well as over an unfunctionalized alkyne. The results obtained with a set of diyne substrates are more compelling (Table 4, entries 7–14): not only did the

### Scheme 9. Intermolecular Competition Experiments



propargylic site react preferentially in all cases investigated, but the *trans*-hydrostannation also outperformed conceivable inter- or intramolecular [2+2] cycloadditions, which are known to be very facile (see above).<sup>11</sup> Moreover, entries 12–14 show that the discrimination between two different acetylene units even

Table 5. *trans*-Hydrometalations of (Hetero)arene Derivatives Endowed with Protic Sites<sup>a</sup>

Entry	Substrate	Reagent	Major product	proximal: distal <sup>b</sup>	Yield (%)
1		Bu <sub>3</sub> SnH		97:3	84
2		BnMe <sub>2</sub> SiH		84:16	97
3		Bu <sub>3</sub> SnH		99:1	85
4		Bu <sub>3</sub> SnH		95:5	78
5		Bu <sub>3</sub> SnH		96:4	79
6		Bu <sub>3</sub> SnH		99:1	90
7		Bu <sub>3</sub> SnH		95:5	81
8		BnMe <sub>2</sub> SiH		99:1	81
9		Et <sub>3</sub> SiH		99:1	65 <sup>c</sup>
10		BnMe <sub>2</sub> SiH		99:1	88
11		Et <sub>3</sub> SiH		99:1	93
12		(Me <sub>3</sub> SiO) <sub>3</sub> SiH		99:1	79
13		(Me <sub>3</sub> SiO) <sub>2</sub> MeSiH		99:1	84
14		Et <sub>3</sub> SiH		99:1	77
15		BnMe <sub>2</sub> SiH		2:98	45 <sup>d</sup>
16		BnMe <sub>2</sub> SiH		99:1	83
17		BnMe <sub>2</sub> SiH		17:83	96

<sup>a</sup>The reactions were carried out at ambient temperature with 1.05–1.2 equiv of R<sub>3</sub>MH in CH<sub>2</sub>Cl<sub>2</sub> in the presence of **1** (1–2 mol %); unless stated otherwise, the selectivity for *trans*-addition was ≥95:5 (major regioisomer). <sup>b</sup>“Proximal” denotes delivery of the R<sub>3</sub>M group to the alkyne C-atom next to the protic group, whereas “distal” refers to the more remote C-atom. <sup>c</sup>The reaction was performed in the presence of B(C<sub>6</sub>F<sub>5</sub>)<sub>3</sub> to block the N-donor site; the additive was then removed on treatment of the crude product with DABCO. <sup>d</sup>Incomplete conversion even after 46 h reaction time.

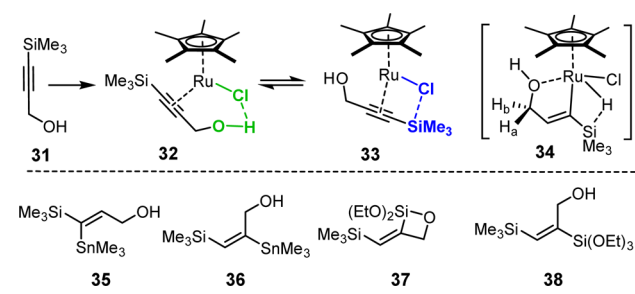
pertains to 1,3-diynes in which the triple bonds are conjugated and hence electronically coupled. The generality of this non-obvious reactivity pattern is currently investigated in more detail and its implementation as a strategic design element into natural product total synthesis is underway.

As mentioned above, even simple arylalkynes such as **23** and **24** proved problematic in the past,<sup>10,11</sup> again most likely because of the ability of an aromatic ring to act as competing four- or even six-electron donor (Scheme 8).<sup>40,41</sup> Therefore, we reinvestigated whether or not a suitably placed protic site allows this severe limitation in substrate scope to be overcome. In line with our expectation, a set of arylalkynes bearing a hydroxyl group or a sulfonamide in the chain underwent *trans*-hydrometalation with ease (Table 5, entries 1–6); the compatibility with a labile aldol motif or an aldehyde underscores the mildness of the method. This favorable outcome suggested that an unprotected –NH group as part of a heterocyclic ring might do the same and force a neighboring triple bond to succumb to *trans*-hydrometalation. Gratifyingly, this proved to be the case even for fairly electron-rich heteroarenes; for reasons of product stability, this study was focused on hydrosilylation, with the different silanes giving largely similar results (entries 7–17). The comparison of entries 10 and 15 is compelling in that the unprotected imidazole derivative reacted much faster than the correspond-

ing less electron-rich N-tosyl derivative; in fact, its hydrosilylation never reached full conversion. Most notably though, the N-unprotected substrate furnished the *trans*/ $\alpha$ -product, whereas its N-tosylated sibling gave the distal isomer. Such a mutually inverse pattern was also seen in the pyridone series (compare entries 16/17); it clearly showcases that silylation at the distal position predominates as soon as the directing effect of the NH group is lost. Of note is also the indole derivative shown in entry 8 that reacted smoothly, whereas a related indazole (entry 9) mandated addition of B(C<sub>6</sub>F<sub>5</sub>)<sub>3</sub> to the mixture to block the high affinity N-donor site (compare the pyridine adduct **17** discussed above); after hydrosilylation, the boron-free product was obtained on treatment of the crude material with DABCO. Collectively, the data compiled in Table 5 substantiate the profound effect that a protic site is able to exert: it allows *trans*-hydrometalation of compounds that are otherwise catalyst poisons to proceed with respectable outcomes and, in so doing, significantly expands the substrate scope of this valuable transformation.

**Limitations: Binding and Reactivity of a TMS-Capped Propargyl Alcohol.** Silylated alkynes make another interesting case, as Me<sub>3</sub>Si– groups are likely non-innocent. While all substrates investigated so far led to single well-defined complexes on treatment with **1**, 3-(trimethylsilyl)prop-2-yn-1-ol (**31**) gives rise to three adducts at –20 °C (Scheme 10); one

## Scheme 10. Binding of a Prototype C-Silylated Propargyl Alcohol



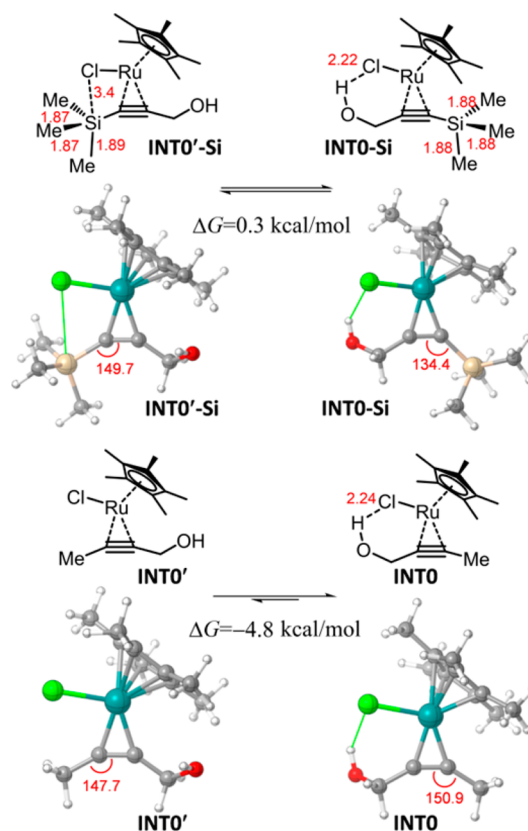
of them (34), however, is likely off cycle.<sup>42</sup> The coordination mode of the major product 32 (ca. 55%) is similar to the one of the propargylic alcohols described above as inferred from the characteristic downfield shift of the alkyne C-atoms ( $\delta_C = 143.0, 95.5$  ppm).

The NMR data of the other relevant complex 33 in solution (ca. 35%,  $\delta_C = 114.6, 92.5$  ppm), however, suggest that the chloride ligand engages with the silyl group which resonates at  $\delta_{Si} = +1.2$  ppm. Such a distinct upfield shift relative to the unbound substrate 31 ( $\delta_{Si} = -17.5$  ppm) is certainly in line with a hypervalent Si...Cl interaction, although it cannot be considered a firm proof.<sup>43,44</sup>

To clarify this interesting aspect, the coordination behavior of the TMS capped propargyl alcohol 31 was explored computationally (Figure 9). The preferred conformations either contain a bridging OH...Cl hydrogen bond (INTO-Si) or what appears to be a hypervalent Si...Cl type interaction (INTO'-Si). There is predicted to be very little difference (0.3 kcal/mol) in energy between the conformers consistent with the experimental observations. Some degree of hypervalent interaction in INTO-Si may be supported by the slight elongation of the pseudoapical Si-Me bond (1.89 Å) relative to the two pseudoequatorial Si-Me bonds (1.87 Å). The Cl-Si bond length is within the sum of their van der Waals radii, suggesting either a steric or bonding interaction. The largest difference however is between the C-C-Si bond angles. The C-C-Si bond angle in INTO-Si is significantly contracted by 15.3° relative to INTO-Si'. The compressed angle in INTO-Si can be attributed to a steric interaction between the methyl groups of the Cp\* and the SiMe<sub>3</sub> moiety which causes an energy increase relative to INTO-Si' thus counteracting the stabilizing effect of the hydrogen bond.

Overall, it is likely a combination of a favorable hypervalent interaction in INTO-Si' and an unfavorable steric interaction in INTO-Si that cancels out the hydrogen bonding in INTO-Si, resulting in nearly equal populations of both conformers. This is in stark contrast to the significant energy difference of 4.8 kcal/mol between the conformers of the nonsilylated complex which is readily attributed to the OH...Cl bond as no hypervalent or steric interaction differences are present. The OH...Cl distances are similar between the nonsilylated and silylated cases suggesting that both have similar bond strengths.

In view of these spectroscopic and computational data, it is not surprising that hydrometalations of compound 31 are hardly selective. Specifically, hydrostannation gave a ~1:1 mixture of 35 and 36. Although hydrosilylation with (EtO)<sub>3</sub>SiH afforded the *trans*/ $\alpha$ -product 37 as the major compound (ca. 57%, spontaneous condensation of the product primarily formed leads to the cyclic siloxane structure), substantial amounts of the *cis*/ $\alpha$ -product 38 are also present in the crude



**Figure 9.** Computed geometries and energy differences for the preferred conformations of the complex between [Cp\*RuCl] and the C-silylated propargyl alcohol 31 versus the complex with 2-butyne. The numbers in red are computed bond distances (Å) and angles (°). The bond angles are displayed on the ball-and-stick rendered models for clarity.

mixture; the question as to why *cis*-adducts are formed at all is not trivial to answer at this point and has to await further studies.

## CONCLUSION

The combined experimental and theoretical approach chosen in this investigation provides a detailed picture of the course of ruthenium catalyzed *trans*-hydrometalation reactions of internal alkynes. Primarily, such substrates behave as four-electron donor ligands to the catalytically active metal fragment [Cp\*RuCl], which entails massive activation of the bound triple bond. Once the reagent R<sub>3</sub>MH (M = Si, Ge, Sn) enters the ligand sphere, the coordinated alkyne switches to assume a two-electron donor character; the resulting loaded complex then evolves via a ruthenacyclopentene as the key intermediate into the final *trans*-addition product. In accordance with the low computed barriers, spectral and preparative data show that the reaction can proceed even at low temperatures. While this explanation for the unorthodox *trans*-selectivity is reminiscent of previous studies on *trans*-hydrosilylation and *trans*-hydrogenation, the current investigation was also able to uncover why unsymmetrical alkynes bearing protic substituents are particularly privileged substrates: a nascent hydrogen bond between the -OH (-NHR) group and the polarized [Ru-Cl] unit leads to tight binding and, at the same time, imposes directionality onto the ligand sphere of the resulting complex, which ultimately accounts for the faithful delivery of the R<sub>3</sub>M-

group to the alkyne C-atom proximal to the steering substituent. Importantly, the cooperativity between protic substituents and catalyst also allows the substrate scope to be significantly expanded: while regular 1,3-enynes or arylalkynes tend to be inert, such compounds react smoothly when carrying an –OH group in vicinity to the triple bond. Even notoriously challenging electron-rich heterocycles prove amenable to *trans*-hydrosilylation, provided they contain an unprotected –NH group as part of the ring system. Finally, the synergy between the [Ru–Cl] unit and a protic group allows site selectivity to be exerted, so that a propargylic triple bond reacts preferentially over a normal alkyne. This roster of enabling features holds significant promise for further applications of alkyne *trans*-addition chemistry.

## ■ ASSOCIATED CONTENT

### Supporting Information

The Supporting Information is available free of charge on the ACS Publications website at DOI: 10.1021/jacs.6b12517.

Experimental part including characterization data, NMR spectra of new compounds, and supporting crystallographic information (PDF)

Computational part including methodological details, orbital interaction data, free energy profile for a regioisomeric pathway, energy tables, and optimized Cartesian coordinates (PDF)

X-ray crystallographic data (CIF)

## ■ AUTHOR INFORMATION

### Corresponding Author

\*fuerstner@kofo.mpg.de

### ORCID

Walter Thiel: 0000-0001-6780-0350

Alois Fürstner: 0000-0003-0098-3417

### Present Addresses

<sup>‡</sup>L.M.W.: Department of Chemistry, University of Massachusetts Lowell, 1 University Avenue, Lowell, MA 01854, USA

<sup>§</sup>M.W.: Indian Institute of Technology Bombay, Mumbai-400076, India

### Notes

The authors declare the following competing financial interest(s): Patent application filed.

## ■ ACKNOWLEDGMENTS

Generous financial support by the Alexander-von-Humboldt Foundation (fellowship to D.A.R.) and the MPG is gratefully acknowledged. We thank the analytical departments of the MPI for excellent support; Dr. J. Flasz, M. Ilg, Dr. M. Müller, Dr. S. Rummelt, Dr. S. Schaubach, Dr. H. Sommer, Dr. F. Ungeheuer for some of the examples shown in the tables; and Umicore AG & Co KG, Hanau, for a generous gift of noble metal salts.

## ■ REFERENCES

(1) (a) Dobbs, A. P.; Chio, F. K. I. In *Comprehensive Organic Synthesis II*, 2nd ed.; Knochel, P., Molander, G. A., Eds.; Elsevier: Amsterdam, 2014; Vol. 8; pp 964–998. (b) Smith, N. D.; Mancuso, J.; Lautens, M. *Chem. Rev.* **2000**, *100*, 3257–3282. (c) *Hydrosilylation. A Comprehensive Review on Recent Advances*; Marciniak, B., Ed.; Advances in Silicon Science 1; Springer: Amsterdam, 2009. (d) Barbeyron, R.; Benedetti, E.; Cossy, J.; Vasseur, J.-J.; Arseniyadis, S.; Smietana, M. *Tetrahedron* **2014**, *70*, 8431–8452.

(2) (a) Trost, B. M.; Ball, Z. T. *J. Am. Chem. Soc.* **2001**, *123*, 12726–12727. (b) Trost, B. M.; Ball, Z. T.; Jöge, T. *J. Am. Chem. Soc.* **2002**, *124*, 7922–7923. (c) Trost, B. M.; Machacek, M. R.; Ball, Z. T. *Org. Lett.* **2003**, *5*, 1895–1898. (d) Trost, B. M.; Ball, Z. T. *J. Am. Chem. Soc.* **2005**, *127*, 17644–17655.

(3) Trost, B. M.; Ball, Z. T. *Synthesis* **2005**, *2005*, 853–887.

(4) Friehe, T. G.; Fürstner, A. *Bull. Chem. Soc. Jpn.* **2016**, *89*, 135–160.

(5) Intramolecularity is arguably the most effective countermeasure; for instructive cases of intramolecular *trans*-hydrosilylations, see: (a) Trost, B. M.; Ball, Z. T. *J. Am. Chem. Soc.* **2003**, *125*, 30–31. (b) Trost, B. M.; Ball, Z. T.; Laemmerhold, K. M. *J. Am. Chem. Soc.* **2005**, *127*, 10028–10038. (c) Denmark, S. E.; Pan, W. *Org. Lett.* **2002**, *4*, 4163–4166. (d) Denmark, S. E.; Pan, W. *Org. Lett.* **2003**, *5*, 1119–1122.

(6) (a) Fürstner, A.; Radkowski, K. *Chem. Commun.* **2002**, 2182–2183. (b) Lacombe, F.; Radkowski, K.; Seidel, G.; Fürstner, A. *Tetrahedron* **2004**, *60*, 7315–7324.

(7) (a) Micoine, K.; Fürstner, A. *J. Am. Chem. Soc.* **2010**, *132*, 14064–14066. (b) Lehr, K.; Mariz, R.; Leseurre, L.; Gabor, B.; Fürstner, A. *Angew. Chem., Int. Ed.* **2011**, *50*, 11373–11377.

(8) The term *trans*-hydrostannation (silylation, germylation) of an alkyne as used herein denotes a reaction in which the H and the MR<sub>3</sub> unit (M = Sn, Si, Ge) end up *trans* to each other. It is pointed out that the resulting product is correctly termed *Z*-configured for the formalism of nomenclature, whereas the product of an analogous *trans*-hydroboration is *E*-configured.

(9) Sundararaju, B.; Fürstner, A. *Angew. Chem., Int. Ed.* **2013**, *52*, 14050–14054.

(10) Rummelt, S. M.; Fürstner, A. *Angew. Chem., Int. Ed.* **2014**, *53*, 3626–3630.

(11) Rummelt, S. M.; Radkowski, K.; Rosca, D.-A.; Fürstner, A. *J. Am. Chem. Soc.* **2015**, *137*, 5506–5519.

(12) (a) Matsuda, T.; Kadowaki, S.; Yamaguchi, Y.; Murakami, M. *Org. Lett.* **2010**, *12*, 1056–1058. (b) Matsuda, T.; Kadowaki, S.; Murakami, M. *Chem. Commun.* **2007**, 2627–2629.

(13) Radkowski, K.; Sundararaju, B.; Fürstner, A. *Angew. Chem., Int. Ed.* **2013**, *52*, 355–360.

(14) Fuchs, M.; Fürstner, A. *Angew. Chem., Int. Ed.* **2015**, *54*, 3978–3982.

(15) Leutzsch, M.; Wolf, L. M.; Gupta, P.; Fuchs, M.; Thiel, W.; Farès, C.; Fürstner, A. *Angew. Chem., Int. Ed.* **2015**, *54*, 12431–12436.

(16) For the first application of the cationic catalyst to propargylic alcohols, see: Trost, B. M.; Ball, Z. T.; Jöge, T. *Angew. Chem., Int. Ed.* **2003**, *42*, 3415–3418.

(17) Similarly directed *trans*-hydroborations of propargyl alcohols have not been achieved because pinacol borane reacts faster with the –OH group than with the triple bond.

(18) Rummelt, S. M.; Preindl, J.; Sommer, H.; Fürstner, A. *Angew. Chem., Int. Ed.* **2015**, *54*, 6241–6245.

(19) (a) Sommer, H.; Fürstner, A. *Org. Lett.* **2016**, *18*, 3210–3213. (b) Schaubach, S.; Fürstner, A.; Michigami, K. *Synthesis* **2016**, 49, 202–208. (c) Sommer, H.; Fürstner, A. *Chem. - Eur. J.* **2017**, *23*, 558–562.

(20) (a) Chung, L. W.; Wu, Y.-D.; Trost, B. M.; Ball, Z. T. *J. Am. Chem. Soc.* **2003**, *125*, 11578–11582. (b) Ding, S.; Song, L.-J.; Chung, L. W.; Zhang, X.; Sun, J.; Wu, Y.-D. *J. Am. Chem. Soc.* **2013**, *135*, 13835–13842. (c) Zhang, X.; Chung, L. W.; Wu, Y.-D. *Acc. Chem. Res.* **2016**, *49*, 1302–1310.

(21) Dutta, B.; Curchod, B. F. E.; Campomanes, P.; Solari, E.; Scopelliti, R.; Rothlisberger, U.; Severin, K. *Chem. - Eur. J.* **2010**, *16*, 8400–8409.

(22) (a) Fagan, P. J.; Mahoney, W. S.; Calabrese, J. C.; Williams, I. D. *Organometallics* **1990**, *9*, 1843–1852. (b) Fagan, P. J.; Ward, M. D.; Calabrese, J. C. *J. Am. Chem. Soc.* **1989**, *111*, 1698–1719.

(23) For pioneering studies, see: (a) Templeton, J. L.; Ward, B. C. *J. Am. Chem. Soc.* **1980**, *102*, 3288–3290. (b) Ward, B. C.; Templeton, J. L. *J. Am. Chem. Soc.* **1980**, *102*, 1532–1538.

- (24) For propargylic alcohols acting as four-electron donors in the osmium series, see: (a) Carbó, J. J.; Crochet, P.; Esteruelas, M. A.; Jean, Y.; Lledós, A.; López, A. M.; Oñate, E. *Organometallics* **2002**, *21*, 305–314. (b) Esteruelas, M. A.; López, A. M.; Ruiz, N.; Tolosa, J. I. *Organometallics* **1997**, *16*, 4657–4667.
- (25) Compare: (a) Le Pailh, J.; Dérien, S.; Bruneau, C.; Demerseman, B.; Toupet, L.; Dixneuf, P. H. *Angew. Chem., Int. Ed.* **2001**, *40*, 2912–2915. (b) Le Pailh, J.; Dérien, S.; Demerseman, B.; Bruneau, C.; Dixneuf, P. H.; Toupet, L.; Dazing, G.; Kirchner, K. *Chem. - Eur. J.* **2005**, *11*, 1312–1324.
- (26) Deuterium bond energies may be lower than hydrogen bond energies, but the effect has previously been estimated to be in the order of only 1–2 kJ/mol (~0.24–0.48 kcal/mol): Rao, C. N. R. *J. Chem. Soc., Faraday Trans. 1* **1975**, *71*, 980–983. Therefore one cannot expect any significant impact on the observed selectivities. In fact, the  $\pi$ -complex formed from a deuterated propargyl alcohol showed the same spectral characteristics (except for the absence of the –OH shift in the  $^1\text{H}$  NMR spectrum) as its protio analogue **4** and identical reactivity in *trans*-hydrostannation and *trans*-hydrosilylation.
- (27) (a) Aullón, G.; Bellamy, D.; Brammer, L.; Bruton, E. A.; Orpen, A. G. *Chem. Commun.* **1998**, 653–654. (b) Kovács, A.; Varga, Z. *Coord. Chem. Rev.* **2006**, *250*, 710–727.
- (28) (a) The average  $\text{C}\equiv\text{C}$  bond length of an alkyne is 1.18 Å, see: Allen, F. H.; Kennard, O.; Watson, D. G.; Brammer, L.; Orpen, A. G.; Taylor, R. *J. Chem. Soc., Perkin Trans. 2* **1987**, S1. (b) The alkyne bond length in a related propynylcyclohexanol derivative is 1.179 Å, see: Robinson, R. P.; Buckbinder, L.; Haugeto, A. I.; McNiff, P. A.; Millham, M. L.; Reese, M. R.; Schaefer, J. F.; Abramov, Y. A.; Bordner, J.; Chantigny, Y. A.; Kleinman, E. F.; Laird, E. R.; Morgan, B. P.; Murray, J. C.; Salter, E. D.; Wessel, M. D.; Yocum, S. A. *J. Med. Chem.* **2009**, *52*, 1731–1743.
- (29) See the [Supporting Information](#) for the methods used for constructing the orbital interaction diagram.
- (30) (a) Trost, B. M.; Livingston, R. C. *J. Am. Chem. Soc.* **1995**, *117*, 9586–9587. (b) Trost, B. M.; Livingston, R. C. *J. Am. Chem. Soc.* **2008**, *130*, 11970–11978.
- (31) For an improved catalyst for redox isomerization, see: Schaubach, S.; Gebauer, K.; Ungeheuer, F.; Hoffmeister, L.; Ilg, M. K.; Wirtz, C.; Fürstner, A. *Chem. - Eur. J.* **2016**, *22*, 8494–8507.
- (32) Despite this rather low affinity, the exchange between bound and unbound substrate is slow; it mandates heating to +50 °C to ensure fast exchange on the NMR time scale.
- (33) Similar interactions have been proposed to serve as regiochemical control elements. For pertinent discussion, see the following and the references cited therein: (a) Trost, B. M.; Ryan, M. C.; Rao, M.; Markovic, T. Z. *J. Am. Chem. Soc.* **2014**, *136*, 17422–17425. (b) Trost, B. M.; Cregg, J. J. *J. Am. Chem. Soc.* **2015**, *137*, 620–623.
- (34) At room temperature, the solution of **5** and MeCN shows the characteristic cherry red color of the alkyne- $\pi$ -complex, whereas it is dark green at –78 °C, which indicates formation of the adduct **5**·MeCN; this process is fully reversible. In the case of pyridine, the line broadening in the NMR spectra of the brown solution at room temperature suggests fast exchange, which is largely frozen out at –78 °C; see the [Supporting Information](#).
- (35) (a) Gutsulyak, D. V.; Churakov, A. V.; Kuzmina, L. G.; Howard, J. A. K.; Nikonov, G. I. *Organometallics* **2009**, *28*, 2655–2657. (b) Osipov, A. L.; Vyboishchikov, S. F.; Dorogov, K. Y.; Kuzmina, L. G.; Howard, J. A. K.; Lemenovskii, D. A.; Nikonov, G. I. *Chem. Commun.* **2005**, 3349–3351.
- (36) Kubas, G. J. *Metal Dihydrogen and  $\sigma$ -Bond Complexes*; Kluwer Academic/Plenum Publishers: Dordrecht, The Netherlands, 2001.
- (37) While stannanes form fairly stable adducts even at ambient temperature (see ref 11), the temperature dependence of the coordination behavior of  $(\text{EtO})_3\text{SiH}$  *vis-à-vis*  $[\text{Cp}^*\text{RuCl}(\text{PiPr}_3)]$  resembles that of MeCN: according to NMR, it is fully coordinated at –80 °C but unbound at room temperature. Associated with this is a characteristic and reversible color change from blue to brown.
- (38) Frohnapfel, D. S.; Templeton, J. L. *Coord. Chem. Rev.* **2000**, 206–207, 199–235.
- (39) See ref 17 and the following: (b) Fagan, P. J.; Ward, M. D.; Calabrese, J. C. *J. Am. Chem. Soc.* **1989**, *111*, 1698–1719. (c) Steines, S.; Englert, U.; Drießen-Hölscher, B. *Chem. Commun.* **2000**, 217–218.
- (40) O'Connor, J. M.; Friese, S. J.; Rodgers, B. L.; Rheingold, A. L.; Zakharov, L. *J. Am. Chem. Soc.* **2005**, *127*, 9346–9347.
- (41) (a) Gill, T. P.; Mann, K. R. *Organometallics* **1982**, *1*, 485–488. (b) Schmid, A.; Piotrowski, H.; Lindel, T. *Eur. J. Inorg. Chem.* **2003**, 2003, 2255–2263.
- (42) The third discrete species in solution (ca. 10%) was identified as the vinylruthenium hydride species **34**, which seems to be a byproduct of the stoichiometric binding experiments and does not play a role in catalysis. The resonance at  $\delta_{\text{H}} = -9.28$  ppm reveals its hydridic nature, whereas the diastereotopicity of the  $\text{CH}_2\text{--OH}$  protons indicates a chelate structure. The shielded  $^{29}\text{Si}$  resonance ( $\delta_{\text{Si}} = +7.6$  ppm) indicates a hypervalent interaction, probably with the hydride ligand. Deuterium labeling experiments suggest that the –OH group of the substrate is the source of the Ru–H unit as well as the alkenyl proton.
- (43) Lachaize, S.; Sabo-Etienne, S. *Eur. J. Inorg. Chem.* **2006**, 2006, 2115–2127.
- (44) See ref 35 and the following: Mai, V. H.; Korobkov, I.; Nikonov, G. I. *Organometallics* **2016**, *35*, 936–942.